Colloid Polym Sci (2009) 287:853–858
DOI 10.1007/s00396-009-2040-1

ORIGINAL CONTRIBUTION

Self-assembled CuO nanoarchitectures and their catalytic activity in the thermal decomposition of ammonium perchlorate

Jun Wang · Shanshan He · Zhanshuang Li · Xiaoyan Jing · Milin Zhang · Zhaohua Jiang

Received: 11 August 2008 / Revised: 18 March 2009 / Accepted: 12 April 2009 / Published online: 1 May 2009

Abstract CuO shuttle-like and flower-like nanocrystals were synthesized through a one-step, low-temperature solution-phase method in the presence of a cation surfactant, hexadecyl trimethyl ammonium bromide. These nanocrystals were studied as an additive for promoting the thermal decomposition of ammonium perchlorate (AP). With the addition of CuO shuttle-like and flower-like nanocrystals, the thermal decomposition temperature of AP decreased. The structure, particle size, and morphology of resulting CuO powders were characterized by X-ray diffraction, scanning electron microscopy, and transmission electron microscopy. Thermogravimetric analysis technique was applied to investigate the thermal decomposition of mixtures of AP and as-prepared CuO nanocrystals.

Keywords Crystal growth · Chemical synthesis · Thermal decomposition · Catalytic activity

Introduction

As a p-type transition metal oxide with a narrow band gap (Eg=1.2 eV), CuO has received considerable attention in recent years due to its exotic properties and wide application, for example, in heterogeneous catalysts [1–3], gas sensors [4], solar cells [5], electrode materials [6–8], superhydrophilic materials [9], and high-T_C superconductors [10]. Besides, significant progress has been made for its application in photochemically active and photoconductive compounds. The nanostructured CuO materials and assemblies have attracted considerable attention in recent years. There have been many reports about the preparation of CuO nanostructures, such as nanorods [5, 8, 11, 12], nanowires [13–15], nanoribbons [11, 13, 16], nanoparticles [17], nanoplatelets [18], nanoneedles [19], nanosheets [6, 20, 21], and nanorings [16]. Apart from these simple shape CuO nanostructures, some complex structures of CuO have also been reported in the literature, such as flower-like structures [22], "Dandelions" structures [23], sheaf-like structures [24], "Honeycombs" structures [25], dendrite-like structures [26], doughnut-like structures [27]. Various methods for the preparation of CuO structures have been investigated, including precursor thermal decomposition [27], hydrothermal methods [12, 18, 26], solid-phase methods [15], wet-chemical methods [11], hydrolysis route [22], electrochemical methods [28].

In our work, CuO shuttle-like and flower-like nanocrystals were synthesized through a one-step, low-temperature solution-phase method in the presence of a cation surfactant, hexadecyl trimethyl ammonium bromide (CTAB). Synthesis of CuO shuttle-like nanocrystals by a hydrothermal route has been reported [29]. The method we reported in this study is a simple, direct, and reproducible synthetic method carried out in a solution phase under mild conditions. The effect of the concentration of surfactant on the shape and structure of CuO crystals was investigated. The possible growth mechanism of CuO shuttle-like and flower-like nanocrystals was discussed. The catalytic activity of the CuO nanocrystals for the decomposition of ammonium perchlorate was examined.

J. Wang · S. He · Z. Li · X. Jing · M. Zhang
College of Material Science and Chemical Engineering,
Harbin Engineering University,
Harbin 150001, People's Republic of China

J. Wang (✉) · Z. Jiang
College of Chemical Engineering, Harbin Institute of Technology,
Harbin 150001, People's Republic of China
e-mail: junwang@hrbeu.edu.cn

Experimental section

Synthesis of sample

Procedure 1

CuO nanostructures were synthesized from the copper nitrate [$Cu(NO_3)_2{\cdot}3H_2O$], hexamethylenetetramine [HMTA; $C_6H_{12}N_4$], and hexadecyl trimethyl ammonium bromide [CTAB; $C_{16}H_{33}(CH_3)_3NBr$] (Beijing Yili Fine Chemicals). All of the chemicals were used as received without further purifications. The experimental procedures are briefly described as follows: The starting solution of copper nitrate (0.1 M) was prepared by dissolving Cu $(NO_3)_2{\cdot}3H_2O$ in distilled water. Typically, 100 mL of the above solution was added to 100 mL aqueous solution of hexamethylenetetramine (0.05 M) with stirring at room temperature, followed by an addition of 0.1 g hexadecyl trimethyl ammonium bromide (CTAB). A few drops of NaOH (aq) were added to adjust the pH to 7.0. The solution was then heated and refluxed under continuous stirring at 100 °C for 3 h in a three-necked refluxing pot. The refluxing temperature of the solution was controlled by inserting a manually adjustable thermocouple in the refluxing pot. After refluxing, the resulting precipitates were washed with distilled water and ethanol and dried in vacuum at 60 °C for 12 h. The product was designated as sample A.

Procedure 2

This was the same as the above procedure apart from the addition of 0.2 g hexadecyl trimethyl ammonium bromide (CTAB) to the solution. The product was designated as sample B.

Characterization of sample

The structure and crystal phases were characterized by power X-ray diffraction (XRD) with Cu Kα radiation, wavelength λ=1.54178 Å (Rigaku D/Max-IIIA). Morphology and structure of CuO were characterized using scanning electron microscopy (SEM, JSM-6480A) and transmission electron microscopy (TEM, PHILIPS CM 200 FEG, 160 kV). The thermal behaviors of the CuO nanocrystals were investigated using a STA 409 PC thermal analyzer at a heating rate of 10 °C min^{-1} from 35 to 450 °C in Argon under ambient pressure.

Catalytic activity measurements

To evaluate the catalytic activity of the as-prepared CuO shuttle-like and flower-like nanocrystals, CuO nanocrystals and NH_4ClO_4 were thoroughly mixed by a grinding method, a thermogravimetric (TG) analysis technique was applied to investigate the thermal decomposition of the mixture (98% NH_4ClO_4–2% CuO, mass percent) from 35 °C to 450 °C under Argon atmosphere. The measurement was performed on a STA 409 PC thermal analyzer with the heating rate of 10 °C min^{-1}.

Results and discussion

Structure and morphology

The composition and phase purity of the as-prepared nanocrystals were examined by powder XRD, which confirmed a high degree of crystallinity with all reflections indexed to the monoclinic CuO (JCPDS card no.48-1548) having cell parameters a=4.688 Å and c=5.132 Å (in Fig. 1a–b). The dominant peaks located at 2θ values between 30° and 80° clearly indicate that the CuO product is a pure phase. No characteristic peaks of impurities such as $Cu(OH)_2$ and Cu_2O were detected.

The morphologies of as-prepared sample A and B were examined by SEM. Figure 2a–b shows the SEM images of shuttle-like CuO nanostructures synthesized in the presence of 0.1 g CTAB. Figure 2c–d shows the SEM image of a single CuO flower synthesized in the presence of 0.2 g CTAB. Figure 2b shows the SEM images of shuttle-like CuO on a large scale. The CuO flower shown in Fig. 2d resembles a blooming flower. A CuO flower is composed of many sheet-like CuO petals, and each of the CuO petals radiates from the center of the crystals to form a flower-like structure. When the mass of the CTAB were increased to 0.25 g, CuO remains as a flower-like structure but

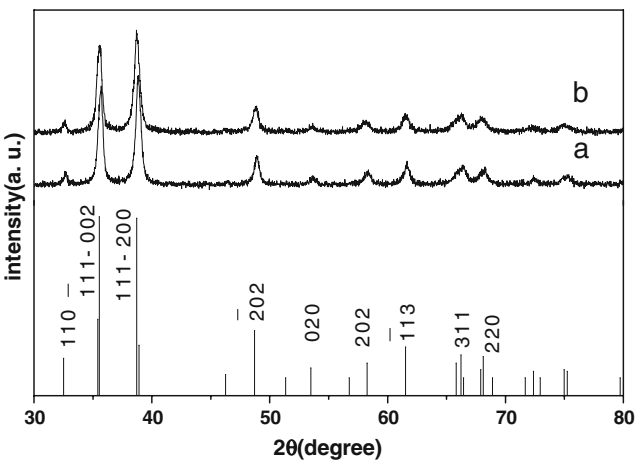

Fig. 1 XRD pattern of the shuttle-like CuO nanostructures. *Vertical lines* represent the standard diffraction data of CuO from JPCDS file (no. 48-1548)

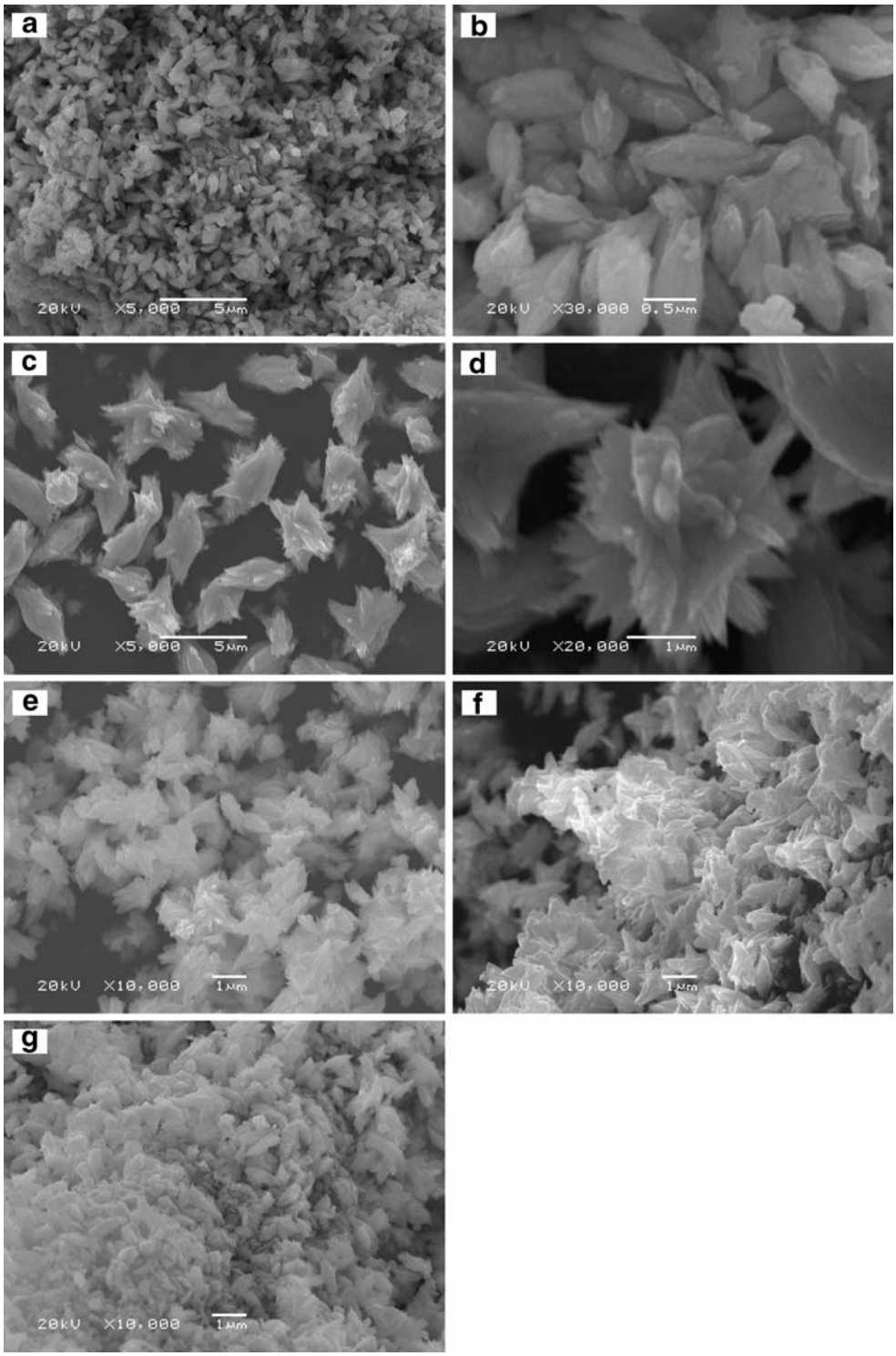

Fig. 2 The SEM image of CuO nanostructures in the presence of the different concentrations of CTAB: **a–b** 0.1 g CTAB; **c–d** 0.2 g CTAB; **e** 0.25 g CTAB; **f** 0.30 g CTAB; **g** 0.00 g CTAB

agglomerates (in Fig. 2e). When the mass of the CTAB were increased to 0.30 g, CuO structure becomes disordered and agglomerates in large area (in Fig. 2f). We also found that in the absence of the surfactant in reaction system, agglomeration of the obtained product still exists (in Fig. 2g). Although the role of CTAB in CuO aggregates growth is still unclear, it is believed that the CTAB molecules play roles in at least two aspects: the role of the dispersion, second, the role of the impact of crystal morphology.

Further structure characterization was carried out by TEM (Fig. 3). The image of an individual shuttle-like CuO is shown in Fig. 3a. It can be seen that the aggregates have breadths of about 300–500 nm and lengths of up to several

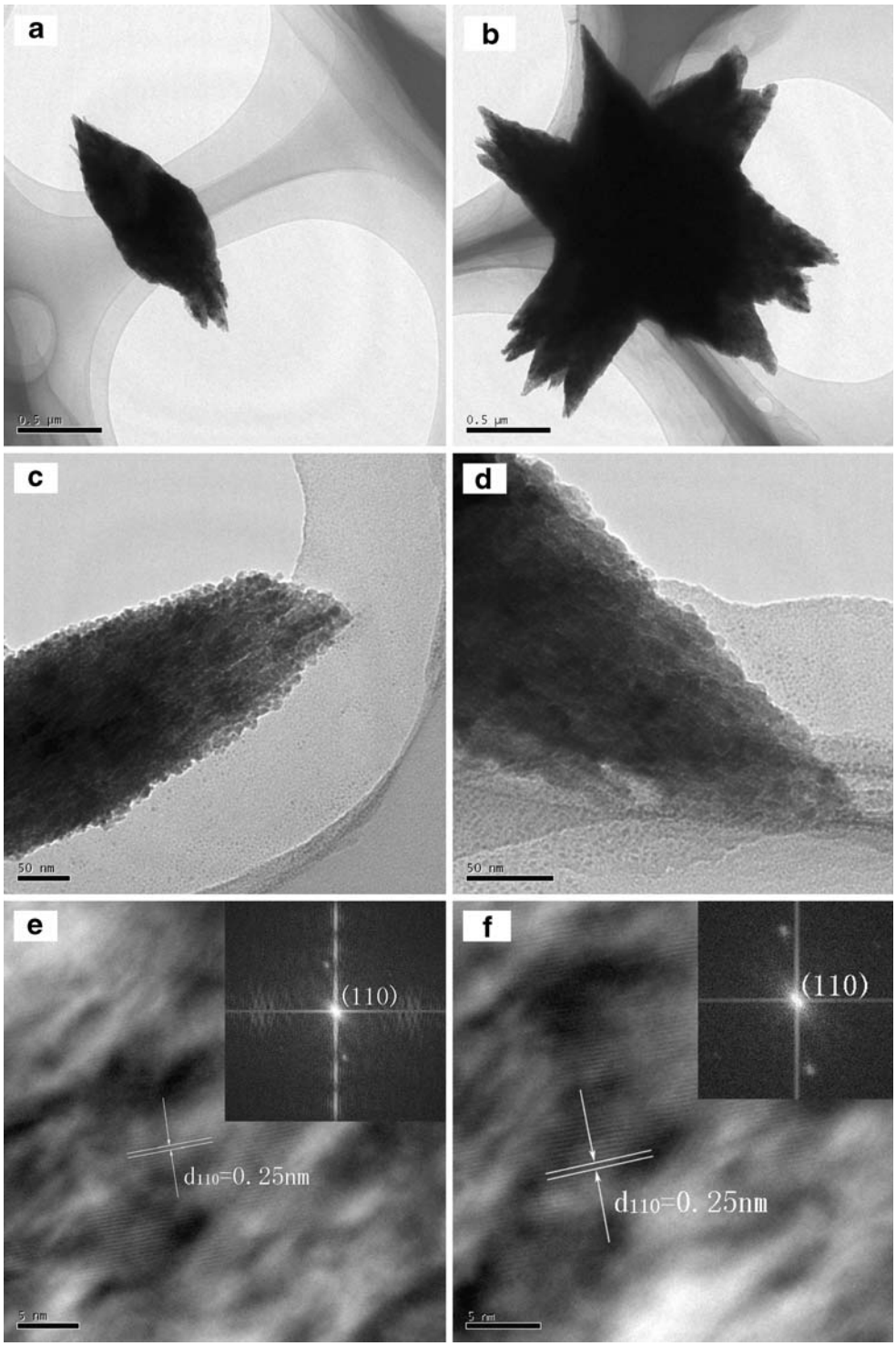

Fig. 3 Low magnification TEM image of the CuO nanostructures: **a** shuttle-like; **b** flower-like; **c** the building blocks of shuttle-like CuO structures; **d** the building blocks of flower-like CuO structures; **e** HRTEM image of the shuttle-like CuO structures, corresponding FFT pattern (*inset*) is consistent with the HRTEM observation; **f** HRTEM image of the flower-like CuO structures, corresponding FFT pattern (*inset*) is consistent with the HRTEM observation

micrometers. The building blocks of shuttle-like CuO structures are mainly composed of numerous nanoparticles (Fig. 3c). The nanoparticles are preferentially aligned perpendicularly to the long axis of the shuttle-like aggregate. Figure 3b shows the low magnification TEM image of the CuO nanoparticles with the flower-like structure. Figure 3d shows the building blocks of flower-like CuO. The structures are mainly composed of numerous nanoparticles. The TEM result is consistent with that of SEM (in Fig. 2b). Figure 3e–f shows the high resolution TEM (HRTEM) image of nanoparticles. The lattice spacing of 0.25 nm corresponds to the *d* spacing of [110] crystal planes. The corresponding FFT pattern (inset in Fig. 3e–f) is consistent with the HRTEM observation.

Catalytic properties of the CuO shuttle-like and flower-like nanostructures

The catalytic activities of CuO shuttle-like and flower-like nanostructures were investigated by thermal decomposition of AP. Figure 4 shows TG curves of pure AP and mixtures of AP with CuO shuttle-like and flower-like nanostructures. The decomposition of pure AP is generally centered at temperatures from 322 °C to 412 °C. Addition of CuO shuttle-like and flower-like nanostructures in AP led to a significant reduction of the terminal decomposition temperature, to 361 °C and 369 °C, respectively.

Growth mechanism of the products

A possible formation mechanism is proposed for the shuttle-like aggregates made by CuO nanocrystals based on the control experimental results in Scheme 1. Shuttle-like and flower-like CuO nanostructures were synthesized by a solution process in the presence of 0.1 g CTAB and 0.2 g CTAB, respectively. The growth of the CuO nanostructures in our case underwent a three-step process: (1) The CuO nanoparticles were formed in the beginning (Fig. 3d); (2) Nanoparticles made up of nanowire aggregated to form the rhombic sheets [23]; (3) The self-organized rhombic sheets gradually transformed themselves into shuttle-like and flower-like nanocrystals facilitated by different initial concentrations of CTAB and the electrostatic attraction of these interparticles [30]. This mechanism is very similar to that of assembly of CuO nanoparticles [31]. Regarding the formation of shuttle-like and flower-like structure, the geometrical shape of building blocks and surfactants must have played a key role. However, more studies are needed to obtain conclusive evidence for the growth of the structures.

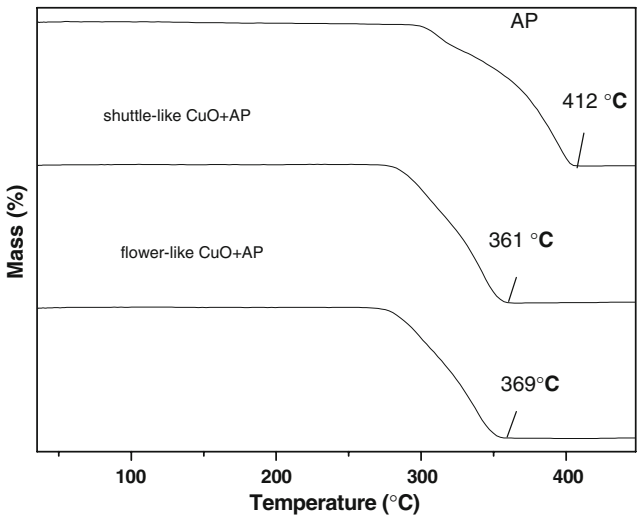

Fig. 4 TG curves for pure AP, mixtures of AP and CuO nanocrystals synthesized in the presence of 0.1 g CTAB and 0.2 g CTAB

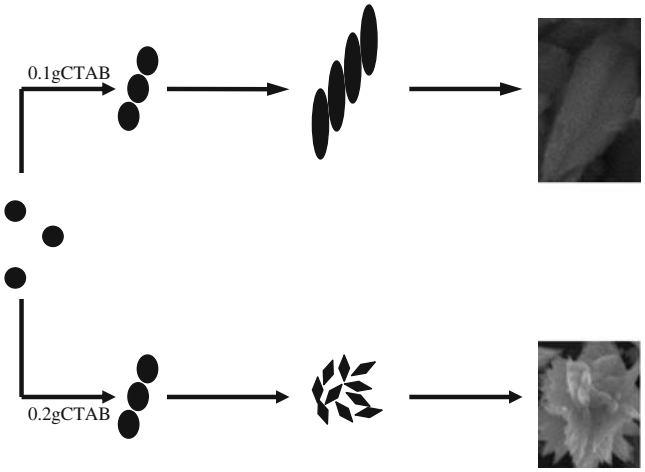

Scheme 1 Illustration of the formation mechanism of shuttle-like and flower-like CuO

Conclusion

CuO shuttle-like and flower-like nanostructures have been fabricated through a simple solution process in the presence of a cation surfactant, hexadecyl trimethyl ammonium bromide (CTAB); experiments show that the self-organized rhombic sheets gradually transform themselves into shuttle-like and flower-like nanocrystals facilitated by different concentrations of CTAB. In addition, the products show an effective catalytic activity for the decomposition of NH_4ClO_4. This synthetic route was simple and reproducible, which might be applied to the preparation of other transition metal oxide nanostructures.

Acknowledgment We gratefully acknowledge the support of this research by the Key Technology R&D program of Heilongjiang Province (no.TB06A05), Science Fund for Young Scholar of Harbin City (no. 2004AFQXJ038), and basic research fund for Harbin Engineering University (no. mzj07076).

References

1. Laxmidhar R, Suribabu JTP (2007) Novel CuO nanoparticle catalyzed C–N cross coupling of amines with iodobenzene. Org Lett 17:3396–3399
2. Zhang MY, Wang LF, Ji HB et al (2007) Cumene liquid oxidation to cumene hydroperoxide over CuO nanoparticle with molecular oxygen under mild condition. J Nat Gas Chem 16:393–398
3. Li XG, Ma BG, Xu L et al (2007) Catalytic effect of metallic oxides on combustion behavior of high ash coal. Energy Fuels 21:2669–2672
4. Zhang JT, Liu JF, Peng Q et al (2006) Nearly monodisperse Cu_2O and CuO nanospheres: preparation and applications for sensitive gas sensors. Chem Mater 18:867–871

5. Sambandam A, Wen XG, Yang SH (2005) Room temperature growth of CuO nanorod arrays on copper and their application as a cathode in dye-sensitized solar cells. Mater Chem Phys 93:35–40
6. Seiichi S, Shogo M, Sinya S et al (2008) Photoelectrochemical characteristics of cells with dyed and undyed nanoporous p-type semiconductor CuO electrodes. J Photochem Photobiol, A Chem 194:143–147
7. Wang SQ, Zhang JY, Chen CH (2007) Dandelion-like hollow microspheres of CuO as anode material for lithium-ion batteries. Scripta Mater 57:337–340
8. Gao XP, Bao JL, Pan GL et al (2004) Preparation and electrochemical performance of polycrystalline and single crystalline CuO nanorods as anode materials for Li ion battery. J Phys Chem B 108:5547–5551
9. Tang KJ, Wang XF, Yan WF et al (2006) Fabrication of superhydrophilic Cu_2O and CuO membranes. J Membr Sci 286:279–284
10. Jarlborg T (2007) Effects of spin–phonon interaction within the CuO plane of high-T_C superconductors. Physical C 454:5–14
11. Chang Y, Zeng HC (2004) Controlled synthesis and self-assembly of single-crystalline CuO nanorods and nanoribbons. Cryst Growth Des 4:397–402
12. Xiao HM, Zhu LP, Liu XM et al (2007) Anomalous ferromagnetic behavior of CuO nanorods synthesized via hydrothermal method. Solid State Commun 141:431–435
13. Du GH, Van Tendeloo G (2004) $Cu(OH)_2$ nanowires, CuO nanowires and CuO nanobelts. Chem Phys Lett 393:64–69
14. Fan XY, Wu ZG, Yan PX et al (2008) Fabrication of well-ordered CuO nanowire arrays by direct oxidation of sputter-deposited Cu_3N film. Mater Lett 62:1805–1808
15. Wang WZ, Zhuang Y, Li L (2008) Structure and size effect of CuO nanowires prepared by low temperature solid-phase process. Mater Lett 62:1724–1726
16. Wang XQ, Xi GC, Xiong SL et al (2007) Solution-phase synthesis of single-crystal CuO nanoribbons and nanorings. Cryst Growth Des 7:930–934
17. Liu XW, Geng BY, Du QB et al (2007) Temperature-controlled self-assembled synthesis of CuO, Cu_2O and Cu nanoparticles through a single-precursor route. Mater Sci Eng 448:7–14
18. Zou GF, Li H, Zhang DW et al (2006) Well-aligned arrays of CuO nanoplatelets. J Phys Chem B 110:1632–1637
19. Liu YL, Liao L, Li JC et al (2007) From copper nanocrystalline to CuO nanoneedle array: synthesis, growth mechanism, and properties. J Phys Chem C 111:5050–5056
20. Al-Kuhaili MF (2008) Characterization of copper oxide thin films deposited by the thermal evaporation of cuprous oxide (Cu_2O). Vacuum 82:623–629
21. Zheng LK, Liu XJ (2007) Solution-phase synthesis of CuO hierarchical nanosheets at near-neutral pH and near-room temperature. Mater Lett 61:2222–2226
22. Zhu JW, Bi HP, Wang YP et al (2007) Synthesis of flower-like CuO nanostructures via a simple hydrolysis route. Mater Lett 61:5236–5238
23. Liu B, Zeng HC (2004) Mesoscale organization of CuO nanoribbons: formation of "Dandelions". J Am Chem Soc 126:8124–8125
24. Zhang M, Xu XD, Zhang ML (2008) Hydrothermal synthesis of sheaf-like CuO via ionic liquids. Mater Lett 62:385–388
25. Liu Y, Chu Y, Zhuo YJ et al (2007) Anion-controlled construction of CuO honeycombs and flowerlike assemblies on copper foils. Cryst Growth Des 7:467–470
26. Zhang H, Li SZ, Ma XY et al (2008) Controllable growth of dendrite-like CuO nanostructures by ethylene glycol assisted hydrothermal process. Mater Res Bull 43:1291–1296
27. Cao AM, Monnell JD, Matranga C et al (2007) Hierarchical nanostructured copper oxide and its application in arsenic removal. J Phys Chem C 11:18624–18628
28. Yuan GQ, Jiang HF, Lin C et al (2007) Shape- and size-controlled electrochemical synthesis of cupric oxide nanocrystals. J Cryst Growth 303:400–406
29. Zhang YG, Wang ST, Li XB et al (2006) CuO shuttle-like nanocrystals synthesized by oriented attachment. J Cryst Growth 291:196–201
30. Li D, Leung YH, Djurišić AB et al (2005) CuO nanostructures prepared by a chemical method. J Cryst Growth 282:105–111
31. Zhang ZP, Sun HP, Shao XQ et al (2005) Three-dimensionally oriented aggregation of a few hundred nanoparticles into monocrystalline architectures. Adv Mater 17:42–47